Continuity from neutron matter to two-flavor quark matter with $^1S_0$ and $^3P_2$ superfluidity

Yuki Fujimoto,[1,*] Kenji Fukushima,[1,2,†] and Wolfram Weise[3,1,‡]

[1]*Department of Physics, The University of Tokyo, 7-3-1 Hongo, Bunkyo-ku, Tokyo 113-0033, Japan*
[2]*Institute for Physics of Intelligence (IPI), The University of Tokyo,*
7-3-1 Hongo, Bunkyo-ku, Tokyo 113-0033, Japan
[3]*Physics Department, Technical University of Munich, 85748 Garching, Germany*

This study is performed with the aim of gaining insights into the possible applicability of the quark-hadron continuity concept, not only in the idealized case of three-flavor symmetric quark matter, but also for the transition from neutron matter to two-flavor quark matter. A key issue is the continuity between neutron superfluidity and a corresponding superfluid quark phase produced by d-quark pairing. Symmetry arguments are developed and relevant dynamical mechanisms are analyzed. It is pointed out that the $^3P_2$ superfluidity in dense neutron matter has a direct analog in the $^3P_2$ pairing of d-quarks in two-flavor quark matter. This observation supports the idea that the quark-hadron continuity hypothesis may be valid for such systems. Possible implications for neutron stars are briefly discussed.

I. INTRODUCTION

Two decades ago a conceptual framework for a continuous connection between hadronic and quark phases of dense matter described by quantum chromodynamics (QCD) was suggested in Ref. [1], based on the exact matching of symmetry breaking patterns and low-lying excitations in both domains. In a similar context, for three-flavor matter, correspondences between condensates of pairs of hadrons and quarks have been discussed in Ref. [2]. These are the foundations for what is called the "quark-hadron continuity" of matter at high baryon density. A Ginzburg-Landau analysis shows that matter at sufficiently low temperature goes through a smooth crossover from the hadronic to the quark phase as one increases the baryon density [3]. Such a continuous crossover is also realized in a three-flavor Nambu–Jona-Lasinio (NJL) model [4]. These features are further borne out by the spectral continuity of Nambu-Goldstone (NG) modes [5] and vector mesons [6]. Recently the continuity of topological defects such as superfluid vortices that appear both in the hadronic phase and the color-flavor locked (CFL) phases have been under discussion [7–9]. A state-of-the-art result based on emergent higher-form symmetry gives a plausible explanation for the quark-hadron vortex continuity to hold even beyond the Ginzburg-Landau regime [10]. Some supplemental arguments for the continuity can be found also in the large-N_C limit (with N_C being the color number) where the color-superconducting gap is suppressed: quarkyonic matter [11] refers to such continuity or duality between nuclear and quark matter. Implications of quarkyonic matter to neutron star physics have been discussed in Ref. [12]. For phenomenology in favor of quarkyonic matter, see recent works [13,14].

Inspired by these theoretical developments, the continuity scenario is now also being considered in the context of neutron stars. Particular examples are the phenomenological constructions of the dense matter equation of state (EoS), with quark-hadron continuity taken into account [15–18]. Conversely, recent attempts to extract the neutron star EoS directly from astrophysical observations, using different methods such as machine learning and Bayesian inference [19–22], may provide a basis for judging the continuity hypothesis.

The above-mentioned continuity concept is so far primarily based on idealized SU(3) flavor symmetric settings. In reality, the strange (s) quark in QCD is much heavier than the up (u) and the down (d) quarks, with a mass ratio $m_s/m_{u,d} \sim 30$. It is therefore more natural to consider isospin-symmetric two-flavor systems rather than starting from three-flavor symmetry.

A prototype example of dense baryonic matter is realized in the interior of neutron stars. Their composition

*[*]fujimoto@nt.phys.s.u-tokyo.ac.jp
[†]fuku@nt.phys.s.u-tokyo.ac.jp
[‡]weise@tum.de

is dominated by neutrons, accompanied by a few percent of protons in β-equilibrium. In the present work we focus on superfluidity in neutron stars (see, e.g., Refs. [23,24] for a review). Under the aspect of quark-hadron continuity, the following issue arises: as one proceeds to high baryon densities, does neutron superfluidity have a corresponding analog at the quark level? The neutrons undergo BCS pairing in a $^1S_0$ state at low baryon densities, i.e., $n_B <$ $0.5n_0$ (with $n_0 \simeq 0.16$ fm^{-3}, the saturation density of normal nuclear matter). This type of superfluid is believed to exist in the inner crust of neutron stars. With increasing baryon density, neutron pairing in the $^3P_2$ state starts to develop and becomes the dominant pairing mechanism for $n_B > n_0$, inward bound towards the neutron star core region. This realization of $^3P_2$ superfluidity is based on the observed pattern of nucleon-nucleon (NN) scattering phase shifts [25,26]. The phase shift of the $^1S_0$ partial wave changes sign from positive to negative with increasing energy of the two nucleons, indicating that the pairing interaction turns from attractive to repulsive with increasing Fermi energy. Consequently, pairing in the $^1S_0$ channel is disfavored at high densities and taken over by pairing in the $^3P_2$ channel. This property is attributed to the significant attraction selectively generated by the spin-orbit interaction in the triplet P-wave with total angular momentum $J = 2$. All other isospin $I = 1$ S- and P-wave NN phase shifts are smaller or repulsive in matter dominated by neutrons. Various aspects and properties of $^3P_2$ superfluidity inside neutron stars, from its role in neutron star cooling to pulsar glitches, are subject to continuing explorations (see, e.g., Refs. [27–29]). A recent advanced analysis of pairing in neutron matter based on chiral effective theory (EFT) interactions including three-body forces can be found in Ref. [30].

Our aim in this work is to investigate the continuity between superfluid neutron matter and two-flavor quark matter with $^1S_0$ and $^3P_2$ superfluidity. Related two-flavor NJL model studies have been reported in Refs. [31,32]. Here our point is to collect and discuss the arguments which do indeed suggest that the continuity concept applies to superfluid pairing when passing from neutron matter to u-d-quark matter with a surplus of d-quarks, as schematically illustrated in Figs. 1 and 2.
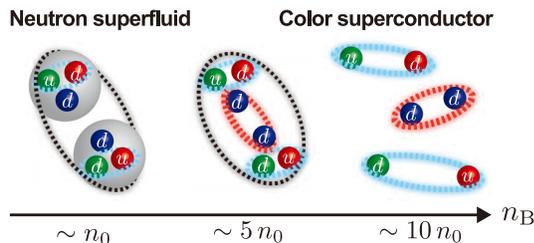

FIG. 1.   Schematic picture of quark-hadron continuity between neutron superfluid and color superconductor. Cooper pairing of neutrons (indicated by dashed line) continuously connects to pairing of quarks in diquark condensates.
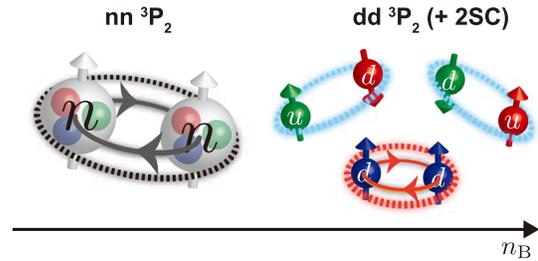

FIG. 2. Schematic picture of quark-hadron continuity between the $^3P_2$ neutron superfluid and the 2SC $+ \langle dd \rangle$ color superconductor.

We emphasize that our continuity concept does not exclude rapid but continuous changes in relevant degrees of freedom. Our focus here is on the logical possibility of a smooth crossover from neutron matter to quark matter. The presumed pattern of phases is as follows. Broken chiral symmetry approaches restoration in highly compressed baryonic matter. As the baryon density increases, the chiral order parameter (i.e., the pion decay constant or, equivalently, the magnitude of the chiral condensate) decreases. Chiral symmetry breaking becomes small in the density region of continuity between nuclear and quark matter but remains nonzero as we discuss the latter: chiral symmetry continues to be *spontaneously* broken. Eventually, at still higher densities, chiral symmetry breaking would be enhanced again once the CFL condensates form.

This paper is organized as follows. In Sec. II we describe some general physical properties of dense neutron star matter and motivate the continuity between hadronic matter and quark matter from a dynamical point of view. Section III recalls the conventional quark-hadron continuity scenario based on symmetry breaking pattern considerations (see Fig. 1). In Sec. IV, we show how the order parameter of $^3P_2$ neutron superfluidity can be rearranged into two-flavor superconducting (2SC) $\langle ud \rangle$ and superfluid $\langle dd \rangle$ diquark condensates (see Fig. 2). Section V clarifies the microscopic mechanism that induces the $\langle dd \rangle$ condensate in the $^3P_2$ state. In Sec. VI A, we demonstrate that the $^3P_2 \langle dd \rangle$ diquark condensate can be related to a macroscopic observable, namely the pressure component of the energy-momentum tensor. This in turn is an important ingredient in neutron star theories. For an isolated nucleon it is also a key subject of deeply virtual Compton scattering measurements at JLab [33]. In Sec. VI B, discussions are followed by a suggestive observation for the necessity of "2SC + X" to fit the cooling pattern, where X may well be identified with the d-quark pairing. Finally, Sec. VII summarizes our findings.

II. ABUNDANCE OF NEUTRONS AND DOWN QUARKS IN NEUTRON STAR MATTER

In the extreme environment realized inside neutron stars, the conditions of β-equilibrium and electric charge

neutrality must be satisfied. A crude but qualitatively acceptable picture is that of a degenerate Fermi gas of protons/neutrons and u, d quarks. Interaction effects will be taken into account later, but let us first consider free particles and briefly overview the qualitative character of the matter under consideration. Here, we assume matter at densities around the onset of u, d quarks where the onset of strangeness degrees of freedom may not occur yet. This assumption is in accordance with the current two-solar-mass pulsar constraints [34].

The β-equilibrium imposes a condition on the chemical potentials of participating particles:

$$\mu_n = \mu_p + \mu_e, \qquad \mu_d = \mu_u + \mu_e, \qquad (1)$$

for the hadronic and the quark phases, respectively. Here μ_e is the chemical potential of the (negatively charged) electrons. Neutrinos decouple and do not contribute to the chemical potential balance. For a given baryon number density, n_B, in the hadronic phase, we have two more conditions for the baryon number density and the electric charge neutrality, namely,

$$n_p + n_n = n_B, \qquad n_p = n_e. \qquad (2)$$

For noninteracting particles the density is related to the chemical potential through

$$n_i = \frac{(\mu_i^2 - m_i^2)^{3/2}}{3\pi^2}, \qquad (3)$$

where i stands for p, n, e in the hadronic phase and for u, d, e in the quark phase. Equations (1)–(3) can then be solved for the three variables, μ_p, μ_n, μ_e, as functions of baryon density n_B.

In a relativistic mean-field picture of strongly interacting matter the interaction effects are incorporated in terms of scalar and vector condensates. The scalar mean field changes the nucleon mass from its vacuum value to a (reduced) in-medium effective mass. The vector mean field shifts the chemical potentials. Here we are not interested in fine-tuning parameters but rather in qualitative features of the Fermi surface mismatch between different particle species. With inclusion of interactions, Eq. (3) is modified with μ_i replaced by the shifted chemical potentials and $m_{p/n}$ by the in-medium masses:

$$\mu_p^* = \mu_p - (G_v + G_\tau)n_p - (G_v - G_\tau)n_n, \qquad (4)$$

$$\mu_n^* = \mu_n - (G_v + G_\tau)n_n - (G_v - G_\tau)n_p, \qquad (5)$$

$$m_{p/n}^* = m_{p/n}\langle\sigma\rangle/f_\pi, \qquad (6)$$

where G_v and G_τ denote the coupling strength parameters of isoscalar and isovector vector fields. For guidance we
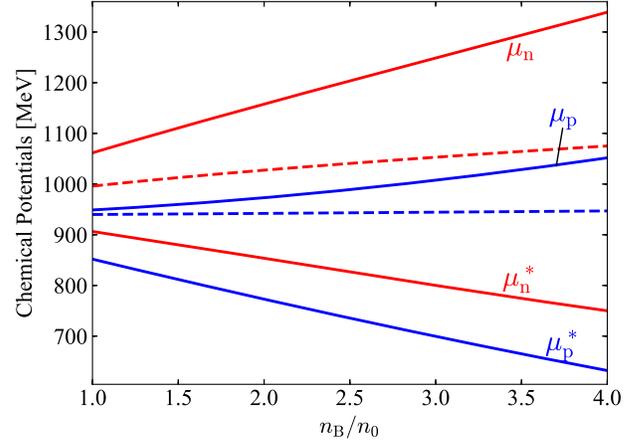

FIG. 3. Nucleon chemical potentials, μ_p, μ_n, μ_p^*, and μ_n^* as functions of the baryon number density n_B normalized by the normal nuclear density n_0. The solid and dashed lines represent results with and without the interaction effects, respectively.

use typical couplings as they emerge in a chiral meson-nucleon field theory combined with functional renormalization group methods, applied to dense nuclear and neutron matter [35]:

$$G_v \sim 4 \text{ fm}^2, \qquad G_\tau \sim 1 \text{ fm}^2. \qquad (7)$$

The scalar mean field $\langle\sigma\rangle$ is normalized to the pion decay constant $f_\pi \simeq 92$ MeV in vacuum and decreases with increasing baryon density. Its detailed density dependence is nonlinear, but for the present discussion it is sufficient to realize that $\langle\sigma\rangle$ drops to about half of its vacuum value at $n_B \sim 5n_0$ (see Fig. 25 of Ref. [35]). So we parametrize the density dependence of the scalar condensate as

$$\langle\sigma\rangle_\mu \simeq \langle\sigma\rangle_0\left(1 - 0.1\frac{n_B}{n_0}\right). \qquad (8)$$

Next we determine μ_p, μ_n, μ_e as functions of n_B. The energy dispersion relations are characterized by the in-medium quantities μ_i^* and m_i^*. The shifted chemical potentials are shown in Fig. 3. Solid lines represent results with inclusion of the interaction effects using the parameters mentioned. The dashed lines are the results with interactions turned off, i.e., using vacuum masses and no shifts on the chemical potentials. In the neutron star environment, μ_n^* is naturally larger than μ_p^*: neutrons dominate the state of matter. Interestingly, the Fermi surface mismatch between neutrons and protons is quite stable with respect to interaction effects, while μ_e is significantly modified.

For quark matter, the corresponding quark chemical potentials are determined by an analogous set of three conditions. Apart from binding energy effects which we neglect here for simplicity, we use constituent quark masses,
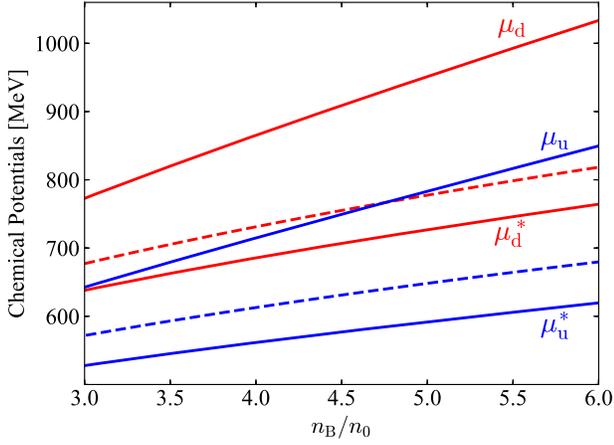
FIG. 4. Quark chemical potentials, μ_u, μ_d, μ_u^*, and μ_d^* as functions of the baryon number density n_B normalized by the normal nuclear density n_0. The solid and dashed lines represent results with and without the interaction effects, respectively.

$$m_u = 312.3 \text{ MeV}, \qquad m_d = 313.6 \text{ MeV}, \qquad (9)$$

fixed to reproduce physical proton and neutron masses, $m_p = 2m_u + m_d$ and $m_n = 2m_d + m_u$. We note that the vector couplings g_v and g_τ in the quark sector should be smaller than G_v and G_τ by 1/9 because of the difference by a factor $N_C = 3$ between baryon and quark number. It is an interesting observation that our input, $g_v \sim G_v/9 = 0.44 \text{ fm}^2$, is suggestively close to a recent estimate [36]: $g_v \sim \pi\alpha_s/(3p_F^2) \sim 0.5 \text{ fm}^2$ (an additional factor of 2 appears here because of a different convention in Ref. [36]). For the density-dependent constituent quark masses we assume the same scaling with $\langle\sigma\rangle$ as for the nucleon mass. In-medium chemical potentials and quark masses are then incorporated as

$$\mu_u^* = \mu_u - (g_v + g_\tau)n_u - (g_v - g_\tau)n_d, \qquad (10)$$

$$\mu_d^* = \mu_d - (g_v + g_\tau)n_d - (g_v - g_\tau)n_u, \qquad (11)$$

$$m_{u/d}^* = m_{u/d}\langle\sigma\rangle/f_\pi. \qquad (12)$$

Figure 4 shows the shifted quark chemical potentials as functions of n_B. In this case again, μ_d^* is naturally larger than μ_u^* for neutron-rich matter in β-equilibrium and under the electric neutrality condition. At high baryon densities this Fermi surface mismatch between d and u quarks shows a correspondence to the mismatch between neutrons and protons in neutron star matter. It suggests the possibility of pairing in the $I = 1$ dd channel analogous to the superfluid neutron pairing mentioned previously.

III. SYMMETRY ARGUMENTS FOR QUARK-HADRON CONTINUITY

Here we give a brief overview of quark-hadron continuity from the symmetry point of view. If the pattern of spontaneous symmetry breaking features a discontinuity between two states or compositions of matter, there must be at least one phase transition separating these two states. This implies that, if two such states are smoothly connected without a phase transition, the symmetry breaking pattern must be identical on both sides. We describe in the following how this symmetry argument works for quark-hadron continuity, first in the three-flavor case and next in the two-flavor case. While the former is well established through the pioneering work of Ref. [1], the latter is a novel scenario that we are proposing in the present work.

A. Three-flavor case

The ground state of three-flavor symmetric quark matter at high density supposedly accommodates diquark condensates featuring a CFL phase. It has been demonstrated that the CFL phase is characterized by the same symmetry breaking pattern as the hadronic phase with a superfluid [1]. Here, diquarks in the color-antitriplet, the flavor-triplet, and the scalar channel, which are often called the "good" diquarks in the context of exotic hadrons (see, e.g., Ref. [37]), play an essential role for the symmetry argument. We thus introduce the corresponding good diquark operator as

$$\hat{\Phi}^{\alpha A} \equiv \mathcal{N}\epsilon^{\alpha\beta\gamma}\epsilon^{ABC}\hat{q}_{\beta B}^\top \mathcal{C}\gamma_5 \hat{q}_{\gamma C}, \qquad (13)$$

where $\mathcal{N}$ is a normalization [38]. In the present study numerical values of superconducting gaps are not essential, so we often omit the normalization factor for simplicity. The charge conjugation matrix, $\mathcal{C} \equiv i\gamma^0\gamma^2$, is inserted to form a Lorentz scalar. In the expression above the spin or Dirac indices are all contracted implicitly. Greek indices (α, β, γ) and capital indices (A, B, C) represent color and flavor, respectively.

In terms of left-handed and right-handed fermions, the diquark operator can be decomposed into $\hat{\Phi}_L^{\alpha A}$ and $\hat{\Phi}_R^{\alpha A}$, respectively. Because diquark condensation in the scalar channel is favored by the axial anomaly, the left- and right-handed condensates, $\Phi_L^{\alpha A} \equiv \langle\hat{\Phi}_L^{\alpha A}\rangle$ and $\Phi_R^{\alpha A} \equiv \langle\hat{\Phi}_R^{\alpha A}\rangle$, in the CFL phase have the property

$$\Phi_L^{\alpha A} = -\Phi_R^{\alpha A} = \delta^{\alpha A}\Delta, \qquad (14)$$

where gauge fixing is assumed so that the color direction aligns with flavor as $\delta^{\alpha A}$, and Δ is a gap parameter.

Clearly $\Phi_L^{\alpha A}$ breaks both flavor $SU(3)_L$ and color $SU(3)_C$, but a simultaneous color-flavor rotation can leave $\Phi_L^{\alpha A}$ unchanged. In the same way $\Phi_R^{\alpha A}$ breaks both flavor $SU(3)_R$ and color $SU(3)_C$ down to their vectorial

combination. This unbroken vectorial symmetry is commonly denoted as $SU(3)_{C+L+R}$. Hence the symmetry breaking pattern can be summarized as $\mathcal{G} \to \mathcal{H}$ with

$$\mathcal{G} = [SU(3)_C] \times SU(3)_L \times SU(3)_R \times U(1)_B,$$
$$\mathcal{H} = SU(3)_{C+L+R}, \tag{15}$$

apart from redundant discrete symmetries. Here $[SU(3)_C]$ represents the global part of color symmetry (while local gauge symmetry is never broken). The spontaneous breaking of global color symmetry makes all eight gluons massive due to the Anderson-Higgs mechanism. It is important to note that $U(1)_B$ corresponding to baryon number conservation is spontaneously broken, so that the CFL state can be regarded as a superfluid. A more detailed discussion on nontrivial realization of the $U(1)_B$ breaking will be given when we consider the two-flavor case in what follows.

The crucial point is now that chiral symmetry breaking (15) in the CFL phase is identical to the familiar scenario in the hadronic phase. The low-energy properties of matter are governed by NG bosons, which implies that chiral EFT can be systematically formulated for the CFL state [39,40]. Therefore the theoretical descriptions of hadronic and CFL matter are analogous by construction. This is the basic message of Ref. [1] which pointed out the important possibility that hadronic and CFL matter can be continuously and indistinguishably connected.

Continuity is a strong hypothesis, requiring a one-to-one correspondence between physical degrees of freedom in hadronic and quark matter. The CFL phase works with quarks, gluons and chiral NG bosons. The spectrum of their excitations can be translated into the relevant composite degrees of freedom in the hadronic phase: nonet baryons, octet vector mesons, and the octet of pseudoscalar NG bosons. Further steps have recently been made investigating the issue of vortex continuity but some controversies still remain.

From the discussions so far one may have thought that $U(1)_B$ is not necessarily broken in the hadronic phase. Surely, on the one hand, the hadronic vacuum at zero density does not break $U(1)_B$. On the other hand, it is known that nuclear matter can have a superfluid component generated by the pairing interaction of nucleons. It is thus conceivable that superfluidity also develops in idealized three-flavor symmetric baryonic matter. We shall return to related considerations in Sec. IV where a superfluid operator for baryons will be explicitly identified.

B. Two-flavor case

The color-flavor-locked configurations assign a special significance to $N_F = N_C = 3$: quark-hadron continuity is usually not postulated for the two-flavor case. In this subsection we point out, however, that such a continuity scenario is also possible for two-flavor nuclear and quark matter. In order for the two-flavor continuity scenario to make sense, the requirements at the quark matter side are: (1) strangeness is negligible; (2) quarks are deconfined and the chiral symmetry is still broken; and (3) baryon superfluidity occurs.

1. 2SC phase

The ground state of two-flavor symmetric quark matter at high density is considered to be the 2SC phase with the following condensates:

$$\Phi_L^{\alpha A} = -\Phi_R^{\alpha A} = \delta^{\alpha 3} \delta^{A3} \Delta. \tag{16}$$

The color direction, $\delta^{\alpha 3}$, is a gauge choice consistent with Eq. (14). These condensates imply a symmetry breaking pattern, $\mathcal{G} \to \mathcal{H}$, with

$$\mathcal{G} = [SU(3)_C] \times SU(2)_L \times SU(2)_R \times U(1)_B,$$
$$\mathcal{H} = [SU(2)_C] \times SU(2)_L \times SU(2)_R \times U(1)_{C+B}. \tag{17}$$

The 2SC condensates partially break the global color symmetry: five out of eight gluons become massive. Since the flavor structure of Eq. (16) is a singlet in the two-flavor sector, chiral symmetry remains intact. Moreover, a modified version of $U(1)_B$ survives unbroken.

To exemplify the unbroken $U(1)_{C+B}$, consider the color-flavor combinations of the pairing underlying Eq. (16). The 2SC phase has nonzero condensates,

$$\langle (ru)(gd) \rangle, \quad \langle (rd)(gu) \rangle, \tag{18}$$

where (ru) denotes a red u quark, etc. Under the $U(1)_B$ transformation, $\hat{q} \to e^{i\theta/3} \hat{q}$, these two pairs receive a phase $e^{2i\theta/3}$ which can be canceled by a color rotation, $\hat{q} \to e^{-i(2/\sqrt{3})\theta T_8} \hat{q}$, with $T_8 = \frac{1}{2\sqrt{3}} \text{diag}(1, 1, -2)$. In the same way we see that the 2SC phase is not an electromagnetic superconductor. The original $U(1)_{em}$ symmetry generated by $Q_e = \text{diag}(\frac{2}{3}, -\frac{1}{3})e$ is broken, but modified $U(1)_{\widetilde{em}}$ remains unbroken which is generated by a mixture of Q_e and T_8,

$$\tilde{Q}_e = Q_e - \frac{e}{\sqrt{3}} T_8. \tag{19}$$

It is therefore evident that the pure 2SC phase itself cannot be smoothly connected to the hadronic phase: symmetry breaking patterns are different. Nevertheless, a coexisting phase is not excluded, in which a chiral condensate $\langle \bar{q}q \rangle$ and diquark condensates (16) are simultaneously nonzero. Coexistence has been confirmed in the preceding model calculations in Refs. [41,42]. Hereafter we assume $\langle \bar{q}q \rangle \neq 0$ in our following discussions. In this way the chiral symmetry breaking part is trivially matched to the

hadronic phase. Below we see that this assumption can be relaxed by an additional condensate.

In contrast to chiral symmetry broken by $\langle \bar{q}q \rangle$, superfluidity is a nontrivial issue. As previously mentioned, the hadronic phase has a superfluid component generated by pairing interactions between nucleons. The quark matter analog should therefore likewise break $U(1)_B$ in order for the continuity scenario to be consistently valid.

2. $2SC + \langle dd \rangle$ phase

As discussed in Sec. II, neutron matter with its maximal isospin asymmetry has an abundance of d quarks which are not paired with u quarks. One can therefore anticipate the formation of a $\langle dd \rangle$ diquark condensate at high baryon densities. The microscopic structure of $\langle dd \rangle$ will be clarified later; for the moment let us consider the simplest case, namely, scalar $\langle dd \rangle$ in the color-sextet channel. On first sight such a condensate appears not to be favored because the one-gluon exchange interaction in the color-sextet channel is repulsive. But it will turn out as we proceed that this repulsive short-distance force is important for the microscopic structure of $\langle dd \rangle$.

Now, if a nonzero $\langle dd \rangle$ in the color-sextet channel coexists in the 2SC phase which may well be called the $2SC + \langle dd \rangle$ phase, we can confirm that $U(1)_B$ symmetry or its modified variants do not survive. The possible color-flavor combinations are

$$\langle (\alpha d)(\beta d) \rangle, \tag{20}$$

where the color pairs are symmetric: $(\alpha, \beta) = (r, r)$, (g, g), (b, b), (r, g), (g, b), (b, r). Under the transformation, $\hat{q} \rightarrow e^{i\theta} e^{-i2\sqrt{3}\theta T_8} \hat{q}$, the pairs $(\alpha, \beta) = (r, r)$, (g, g), (r, g) are invariant, but the remaining three combinations change nontrivially. If we consider continuity from neutron matter, $(\alpha, \beta) = (b, b)$ is favored since ud diquarks are chosen as Eq. (16) in a gauge-fixed description of the 2SC phase. Thus, the $2SC + \langle dd \rangle$ phase breaks $U(1)_B$ and exhibits superfluidity. Also, $\langle dd \rangle$ induces the chiral symmetry breaking even without the chiral condensate. This $\langle dd \rangle$ fulfills the desired properties for the quark-hadron continuity to be valid, which are lacking in the pure 2SC phase. The dynamical aspect of the chiral symmetry breaking in a certain model deserves further consideration as a future work. Here we note that the single-color and single-flavor pairing such as $\langle (bd)(bd) \rangle$ has been studied in the preceding work [43].

Finally, before closing our symmetry argument for quark-hadron continuity, we note that modified electromagnetic $U(1)_{\widetilde{em}}$ remains unbroken, so the $2SC + \langle dd \rangle$ phase cannot be an electromagnetic superconductor. To confirm this, the quickest way is that (bd) quarks, dominant constituents in $\langle dd \rangle$, are neutral with respect to $\tilde{Q}_e$. Therefore, $\langle dd \rangle$ does not affect the $U(1)_{\widetilde{em}}$

symmetry. The charge properties of the (bu) and (bd) quarks in the 2SC were explicitly given in Ref. [44].

In the CFL phase, (bu) and (bd) quarks are identified with protons and neutrons, respectively [2], thus it is also natural to expect the neutron condensate $\langle nn \rangle$ maps to $\langle (bd)(bd) \rangle$ condensate in the 2SC phase. It is also worth mentioning that $\langle (bu)(bu) \rangle$ breaks the $U(1)_{\widetilde{em}}$ symmetry, which is consonant with the fact that the $\langle pp \rangle$ condensate induces the proton superconductivity.

Even with $\langle dd \rangle$ condensation, there remain unpaired quarks in the $2SC + \langle dd \rangle$ phase. These unpaired quarks do not affect the continuity but may dominate low energy excitations, which may eventually be suppressed by dynamical symmetry breaking.

IV. REARRANGEMENT OF THE ORDER-PARAMETER OPERATORS

The following exercise is to formally demonstrate quark-hadron continuity using gauge-invariant order parameters. An essential observation for the intuitive understanding of quark-hadron continuity lies in the fact that no physical or gauge-invariant quantity can discriminate nuclear and quark matter. This observation is traced back to the absence of any order parameter for deconfinement of dynamical quarks in the color fundamental representation.

Throughout this work we describe the low-lying baryons in terms of a quark-diquark structure; for our purpose matching of the right quantum number is sufficient. In this picture the colorless spin-$\frac{1}{2}$ baryon operators, with flavor indices A, B shown explicitly, are given by

$$\hat{\mathcal{B}}_\sigma^{AB} = \hat{\Phi}^{\alpha A} \hat{q}_{\alpha\sigma}^B, \tag{21}$$

where σ denotes the spin index. We note again that the normalization is dropped for notational brevity. This baryon interpolating operator may well have the largest overlap with the physical state, so such a combination of quark-diquark can be regarded as a reasonable approximation for baryon wave functions. In any case, as long as we consider the quark-hadron continuity, what really matters is the quantum number only.

A. Three-flavor symmetric case

Here we start with the order parameters in the CFL phase which are then translated into the hadronic representation. The gauge-invariant order parameters are the mesonic and the baryonic condensates defined as

$$\mathcal{M}^{AB} = \langle \hat{\mathcal{M}}^{AB} \rangle = \langle \hat{\Phi}^{\dagger A\alpha} \hat{\Phi}^{\alpha B} \rangle, \tag{22}$$

$$\Upsilon^{ABC} = \langle \hat{\Upsilon}_{CFL}^{ABC} \rangle = \langle \epsilon^{\alpha\beta\gamma} \hat{\Phi}^{\alpha A} \hat{\Phi}^{\beta B} \hat{\Phi}^{\gamma C} \rangle, \tag{23}$$

respectively. We are primarily interested in superfluidity aspects and hence focus on $\hat{\Upsilon}^{ABC}$. Decomposing $\hat{\Phi}^{\alpha A}$ into

quarks and combining the quark operators with the remaining $\hat{\Phi}^{\beta B}$ and $\hat{\Phi}^{\gamma C}$ to form two-baryon operators, one arrives at

$$\hat{\Upsilon}^{ABC} = 2\epsilon^{AMN}\hat{\mathcal{B}}_{\sigma}^{BM}(\mathcal{C}\gamma_5)_{\sigma\sigma'}\hat{\mathcal{B}}_{\sigma'}^{CN}. \tag{24}$$

Let us now limit ourselves to the octet baryons:

$$\mathcal{B}_{\mathbf{8}}^{AB} = \begin{pmatrix} \frac{1}{\sqrt{2}}\Sigma^0 + \frac{1}{\sqrt{6}}\Lambda & \Sigma^+ & p \\ \Sigma^- & -\frac{1}{\sqrt{2}}\Sigma^0 + \frac{1}{\sqrt{6}}\Lambda & n \\ \Xi^- & \Xi^0 & -\frac{2}{\sqrt{6}}\Lambda \end{pmatrix}_{AB}, \tag{25}$$

where $(\mathcal{C}\gamma_5)^{\top} = -\mathcal{C}\gamma_5$ is used with $\top$ denoting the transpose. Thus, the flavor-singlet CFL order parameter, $\Upsilon^{(0)} \equiv \epsilon^{ABC}\Upsilon^{ABC}$, is smoothly connected to superfluid strange baryonic matter, explicitly represented as

$$\Upsilon^{(0)} = 2(\mathcal{C}\gamma_5)_{\sigma\sigma'}\langle\hat{\mathcal{B}}_{\mathbf{8}\sigma}^{AA}\hat{\mathcal{B}}_{\mathbf{8}\sigma'}^{BB} - \hat{\mathcal{B}}_{\mathbf{8}\sigma}^{AB}\hat{\mathcal{B}}_{\mathbf{8}\sigma'}^{BA}\rangle$$

$$\propto (\mathcal{C}\gamma_5)_{\sigma\sigma'}\left\langle\frac{1}{2}\Lambda_\sigma\Lambda_{\sigma'} + \frac{1}{2}\Sigma_\sigma^0\Sigma_{\sigma'}^0 + \Sigma_\sigma^+\Sigma_{\sigma'}^-\right.$$

$$\left. + p_\sigma\Xi_{\sigma'}^- + n_\sigma\Xi_{\sigma'}^0\right\rangle. \tag{26}$$

At this point we consider the nonrelativistic reduction of the dibaryonic condensates. Conventionally the $^3P_2$ neutron superfluidity has been discussed in the nonrelativistic regime, so it is useful to see what the relativistic counterpart of the nonrelativistic condensates is. The term $\langle\Lambda\Lambda\rangle$ may serve as a specific example. The generalization to other terms is straightforward. Using a solution of the Dirac equation with γ^μ in the Dirac representation, the four-component spinor of the Λ is expressed as

$$\Lambda = \begin{pmatrix} \varphi_\Lambda \\ \frac{\sigma \cdot p}{E_p + m_\Lambda}\varphi_\Lambda \end{pmatrix}, \tag{27}$$

with two-component spinors φ_Λ. The lower components are negligible in the limit $m_\Lambda \gg |p|$ and one finds

$$(\mathcal{C}\gamma_5)_{\sigma\sigma'}\langle\Lambda_\sigma\Lambda_{\sigma'}\rangle = \langle\varphi_\Lambda^{\top}i\sigma^2\varphi_\Lambda\rangle, \tag{28}$$

in terms of the nonrelativistic wave function φ_Λ whose two components correspond to the spin degrees of freedom.

B. Two-flavor $^1S_0$ superfluid matter

The preceding subsection started by identifying the ground state as quark matter in the CFL phase followed by the rearrangement of order parameters in terms of baryonic operators. For the two-flavor case we follow an inverse sequence of steps: the starting point is now neutron matter with a superfluid component and we investigate the

possibility of a continuous transition to superfluid quark matter with an excess of d-quarks.

As long as the baryon density is below the onset of P-wave superfluidity, the neutron superfluid occurs in the $^1S_0$ channel. In this case the superfluid order parameter in neutron matter is given by $\langle\varphi_n^{\top}i\sigma^2\varphi_n\rangle$ in the nonrelativistic representation [see Eq. (28)], which can be generalized into a relativistic expression as

$$\langle\varphi_n^{\top}i\sigma^2\varphi_n\rangle \rightarrow \langle\hat{\Upsilon}_S\rangle \equiv \langle\hat{n}_\sigma(\mathcal{C}\gamma_5)_{\sigma\sigma'}\hat{n}_{\sigma'}\rangle. \tag{29}$$

The relativistic neutron operator, $\hat{n}$, can be written in terms of its composition of udd quarks, i.e.,

$$\hat{n}_\sigma = \epsilon^{\alpha\beta\gamma}(\hat{u}_\alpha^{\top}\mathcal{C}\gamma_5\hat{d}_\beta)\hat{d}_{\gamma\sigma} = \hat{\Phi}_{ud}^{\gamma}\hat{d}_{\gamma\sigma}, \tag{30}$$

where we have introduced the good two-flavor diquark operator, $\hat{\Phi}_{ud}^{\gamma} \equiv \epsilon^{\alpha\beta\gamma}\hat{u}_\alpha^{\top}\mathcal{C}\gamma_5\hat{d}_\beta$ [cf. Eqs. (13) and (16)].

It is then straightforward to rearrange the indices and factorize $\Upsilon_S \equiv \langle\hat{\Upsilon}_S\rangle$ into diquark condensates as

$$\Upsilon_S = \langle\hat{\Phi}_{ud}^\alpha\hat{\Phi}_{ud}^\beta\hat{d}_\alpha^{\top}\mathcal{C}\gamma_5\hat{d}_\beta\rangle \approx \Phi_{ud}^\alpha\Phi_{ud}^\beta\langle\hat{d}_\alpha^{\top}\mathcal{C}\gamma_5\hat{d}_\beta\rangle. \tag{31}$$

At high densities where the physical degrees of freedom are dominated by quarks and the antitriplet diquark condensate develops, Υ_S should be largely given by the right-hand side in a sense of a standard mean-field approximation; we transform the gauge-variant diquark field by introducing the fluctuation from its mean value, and neglect the higher order fluctuation term. Here, we assumed unitary gauge fixing to make our discussion clear. From the expression (31) we see that a scalar $\langle dd\rangle$ condensate is induced in a scenario that smoothly connects superfluid neutron matter to quark matter. The condensate $\langle dd\rangle$ is symmetric in flavor and antisymmetric in spin, and hence symmetric in the color indices α, β. This means that the permitted color structure belongs to the sextet representation. As previously argued in Sec. III, $\langle dd\rangle$ breaks U(1)$_B$ and therefore exhibits S-wave superfluidity. In essence, the neutron superfluid is transformed continuously into the d-quark superfluid.

C. Two-flavor $^3P_2$ superfluid matter

For P-wave superfluidity the quark-hadron continuity argument proceeds in a similar way. We start by writing down the pairing operator of two neutrons in the $S = 1$ and $L = 1$ channel as

$$\varphi_n^{\top}\sigma^2\sigma^i\nabla^j\varphi_n, \tag{32}$$

where the indices i and j run over spatial coordinates x, y, and z.

Now, to address continuity from neutron matter to quark matter, we need to generalize the pairing operator into a relativistic form. This generalization may not be unique; some part of the spatial derivative can emerge from the

lower component of the spinor (27). The only boundary condition is to recover Eq. (32) in the nonrelativistic limit, and it is of course desirable to adopt expressions that are as simple as possible. One such candidate is

$$\varphi_n^\top \sigma^2 \sigma^i \nabla^j \varphi_n \to \hat{\Upsilon}_P^{ij} \equiv \hat{n}^\top C\gamma^i \nabla^j \hat{n}. \quad (33)$$

With this operator, the index structures for the $^3P_0$, $^3P_1$, and $^3P_2$ channels can be further classified as follows:

$$^3P_0 : \hat{\Upsilon}_{P_0} = \hat{\Upsilon}_P^{ii}, \quad (34)$$

$$^3P_1 : \hat{\Upsilon}_{P_1}^i = \epsilon^{ijk} \hat{\Upsilon}_P^{jk}, \quad (35)$$

$$^3P_2 : \hat{\Upsilon}_{P_2}^{ij} = \hat{\Upsilon}_P^{ij} - \frac{1}{3}\delta^{ij}\hat{\Upsilon}_{P_0}. \quad (36)$$

The expression of the $^3P_2$ operator above is in consonance with the general form of the gap matrix for $J = 2$ pairing [45]. As we argued before, at sufficiently high baryon density the $^3P_2$ state is favored.

Simple algebra as in the previous subsection then leads to the rearrangement of the operators from neutrons to diquarks as follows:

$$\Upsilon_P^{ij} = \langle \hat{\Upsilon}_P^{ij} \rangle$$
$$\approx \Phi_{ud}^\alpha (\nabla^j \Phi_{ud}^\beta) \langle \hat{d}_\alpha^\top C\gamma^i \hat{d}_\beta \rangle + \Phi_{ud}^\alpha \Phi_{ud}^\beta \langle \hat{d}_\alpha^\top C\gamma^i \nabla^j \hat{d}_\beta \rangle. \quad (37)$$

Here the first term proportional to $\nabla\Phi_{ud}^\beta$ can be nonzero if the ground state develops a crystalline color-superconducting phase in which the Cooper pair carries a finite net momentum. It is an interesting problem how to optimize a possible interplay between the crystalline profile and the spin-1 condensate $\langle d\gamma^i d \rangle$, but we postpone this discussion and leave such a possibility for a future study.

In this work we concentrate on the second term involving $\langle d\gamma^i \nabla^j d \rangle$. It is now evident that the $^3P_2$ nature of neutron superfluidity is translated to that of d quarks with their color configuration coupled to the scalar diquark condensates in Eq. (37). As in the case of $^1S_0$ superfluidity, this tensorial $\langle d\gamma^i \nabla^j d \rangle$ condensate would also retain the baryon superfluidity. The symmetry breaking patterns on both sides of neutron and quark matter become exactly the same. The remaining step is now to understand the dynamics that favors $^3P_2$ over $^1S_0$ pairing with increasing baryon density.

V. DYNAMICAL PROPERTIES FAVORING TRIPLET P-WAVE PAIRING

Next we analyze dynamical mechanisms for $^3P_2$ pairing in the dd channel. This dynamical consideration is aimed to establish the quark-hadron continuity and to match the quantum number of angular momentum to the neutron superfluid, which also carries the $^3P_2$ angular momentum quantum number. We first discuss why P-wave pairing is

preferred instead of S-wave pairing. Then the role of the spin-orbit interaction in favoring the $J = 2$ state among the $^3P_{J=0,1,2}$ channels will be clarified.

A. Short-range repulsive core favoring $L = 1$

Dense neutron matter is strongly affected by the short-distance dynamics of the NN interaction. At low densities, the attractive $^1S_0$ interaction dominates, while the P-wave ($L = 1$) interaction takes over at higher densities. The short-range repulsion in the $^1S_0$ channel acts to change the sign of the effective nn interaction at the Fermi surface, from attractive to repulsive at densities $n_B \gtrsim 0.5n_0$. The $^1S_0$ pairing becomes disfavored as compared to P-wave pairing. The question is now whether an analogous short-distance repulsive mechanism can be identified in the interaction between two d-quarks.

At very high densities where a perturbative QCD treatment is feasible, the quark scattering amplitude is well described by one-gluon exchange with the following color structure:

$$\sum_{\mathcal{A}=1}^{8} T_{\alpha\alpha'}^{\mathcal{A}} T_{\beta\beta'}^{\mathcal{A}} = -\frac{1}{3}(\delta_{\alpha\alpha'}\delta_{\beta\beta'} - \delta_{\alpha\beta'}\delta_{\alpha'\beta})$$
$$+ \frac{1}{6}(\delta_{\alpha\alpha'}\delta_{\beta\beta'} + \delta_{\alpha\beta'}\delta_{\alpha'\beta}), \quad (38)$$

where $T^{\mathcal{A}}$'s are the color SU(3) generators ($\mathcal{A} = 1, \ldots, 8$). The first term corresponds to the attractive $\bar{\mathbf{3}}_A$ channel, whereas the second term corresponds to the repulsive $\mathbf{6}_S$ channel. The color structure of our dd condensate is in fact in the symmetric color sextet representation. Therefore, in the perturbative region, the short-range part of the interaction between d quarks is repulsive and naturally disfavors S-wave pairing.

In the confined phase, a short-distance repulsive interaction between quarks can be thought of as emerging from quark-gluon exchange in a nonrelativistic quark model picture (cf. the sketch in the middle of Fig. 1). Indeed it has been shown that the short-range repulsive core in the $^1S_0$ channel of the nucleon-nucleon interaction arises from the combined action of the Pauli principle and the spin-spin force between quarks [46,47]. Using the resonating group method, the scattering phase shifts between two nucleons in S-wave were calculated and turned out to be negative (see Fig. 2 of Ref. [46]). We show now that this mechanism correctly accounts for the short-distance repulsive behavior of the interaction between two d-quarks.

In the nonrelativistic quark model analysis of the interaction between two nucleons, one needs to consider only single quark exchange with spin-spin correlation. Two- or three-quark exchange processes are redundant modulo exchange of the two nucleons. For two interacting neutrons, assuming $\langle ud \rangle$ pairing in 2SC configurations (see Sec. III B), one can therefore focus on the exchange
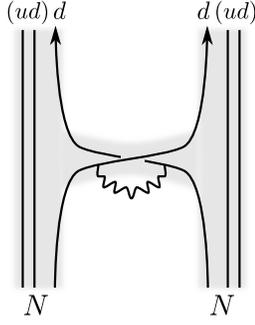
FIG. 5. Short-range interaction between neutrons mediated by quark-gluon exchange.

interaction between the two d-quarks and construct the dd potential as illustrated in Fig. 5: two d quarks cross their lines in the presence of an exchanged gluon. Direct gluon exchange without quark exchange is not allowed because of color selection rules. The one-gluon exchange (OGE) potential reads [48]

$$V_{12}^{\text{OGE}} = \left(\sum_A T_1^A T_2^A \right) \frac{\alpha_s}{4} \left[\frac{1}{r_{12}} - \frac{2\pi}{3m_q^2} (s_1 \cdot s_2) \delta^3(r_{12}) \right], \quad (39)$$

omitting the tensor term in this expression. Here r_{12} denotes the distance between quarks 1 and 2. Their spin operators are denoted by s_1 and s_2. The color structure in front of the potential is exactly the same as the representation in Eq. (38). In close analogy with the nn interaction, short-range repulsion appears in the dd potential. Therefore pairing in $L = 0$ is disfavored and superfluidity appears predominantly in the $L = 1$ state.

B. Spin-orbit interaction favoring $J = 2$

The previous discussion has pointed to dd quark pairing in ^3P_J states. While the spin triplet necessarily follows in $L = 1$ states from the statistics of the wave function, the total angular momentum J is still left unspecified.

In neutron star matter, $^3P_2$ neutron superfluidity occurs because of the strong spin-orbit interaction between neutrons. The matrix elements of

$$L \cdot S = \frac{1}{2} [J(J+1) - L(L+1) - S(S+1)] \quad (40)$$

are $-2, -1$ and $+1$ in $^3P_0$, $^3P_1$ and $^3P_2$ states, respectively. With an extra minus sign in the spin-orbit potential, there is attraction in $^3P_2$ and repulsion in $^3P_{J=0,1}$ channels. These features are also reflected in the empirical triplet P-wave phase shifts. The tensor force in $^3P_2$ is relatively weak: 10 times smaller than the one in the $^3P_0$ channel. In the absence of the spin-orbit force, superfluidity would in fact appear in $^3P_0$.

The neutron-neutron spin-orbit interaction is generated by Lorentz scalar and vector couplings of the neutrons.

In chiral theories, such couplings involve two- and three-pion exchange mechanisms. Phenomenological boson exchange models [49,50] associate these interactions with scalar and vector boson fields, $\sigma(x)$ and $v^\mu(x)$. The vector field includes isoscalar and isovector terms (sometimes identified with ω and ρ mesons, but ultimately representing multipion exchange mechanisms together with short-distance dynamics). In the neutron-neutron interaction the isoscalar and isovector terms have the same weight (the extra factor in the isovector part is $\tau_1 \cdot \tau_2 = 1$).

We start from the following boson-nucleon vertex Lagrangians:

$$\mathcal{L}_S = -g_S \bar{\psi}(x)\psi(x)\sigma(x),$$
$$\mathcal{L}_V = -g_V \bar{\psi}(x)\gamma_\mu \psi(x) v^\mu(x)$$
$$+ \frac{g_T}{2m_N} \bar{\psi}(x)\sigma_{\mu\nu}\psi(x)\partial^\nu v^\mu(x), \quad (41)$$

where m_N is the nucleon mass. Scalar and vector boson masses will be denoted by m_S and m_V. Next, consider the momentum space matrix elements of nucleon-nucleon t-channel Born terms generated by these vertices and identify their spin-orbit pieces. In the NN center-of-mass frame, introduce initial and final state momenta, p and p', and total spin $S = s_1 + s_2$. Furthermore,

$$P = \frac{1}{2}(p + p'), \qquad q = p' - p. \quad (42)$$

The spin-orbit interaction matrix element deduced from interactions in Eq. (41) to (leading) order p^2/m_N^2 is

$$\langle p'|V_{LS}|p \rangle = -\frac{i}{2m_N^2} \left[\frac{g_S^2}{q^2 + m_S^2} + \frac{3g_V^2 + 4g_V g_T}{q^2 + m_V^2} \right] S \cdot (P \times q). \quad (43)$$

We note that upon Fourier transformation, Eq. (43) turns into the r-space spin-orbit potential,

$$V_{LS}(r) = \frac{1}{2m_N^2 r} \frac{df(r)}{dr} L \cdot S,$$
$$f(r) = \frac{g_S^2}{4\pi} \frac{e^{-m_S r}}{r} + \frac{g_V^2}{4\pi} \left(3 + \frac{4g_T}{g_V} \right) \frac{e^{-m_V r}}{r}, \quad (44)$$

with $L = r \times P$. For $\langle L \cdot S \rangle = +1$ in the $^3P_2$ channel, the spin-orbit potential is *attractive* since $d/dr(e^{-mr}/r) = -(1 + mr)e^{-mr}/r^2 < 0$.

Let us make a quick estimate of the magnitude of the $L \cdot S$ force at a distance $r \sim 1$ fm between two nucleons. The isoscalar coupling parameters are, roughly, $g_S^2/4\pi \sim 8$ together with $g_V \simeq g_S$ and $g_T \simeq 0$. The isovector vector interaction has $g_V^2/4\pi \simeq 0.5$ and $g_T/g_V \simeq 6$ (with contributions from isoscalar and isovector vector interactions to

be added in $I = 1$ states such as two neutrons). Using boson masses $m_S \sim 0.5$ GeV and $m_V \sim 0.8$ GeV, this gives in the neutron-neutron $^3P_2$ channel

$$V_{LS}^{nn}(r \sim 1 \text{ fm}) \simeq -24 \text{ MeV}, \tag{45}$$

which is a characteristic order-of-magnitude documented by nuclear phenomenology. Recall that an average distance of about 1 fm between nucleons corresponds to densities 5–6 times the density of normal nuclear matter, so it is already representative of the situation in neutron star cores.

Now consider by analogy a corresponding scenario in terms of quarks, i.e., we wish to examine $^3P_2$ superfluidity in the context of hadron-quark continuity. We seek possible mechanisms that generate an $\boldsymbol{L} \cdot \boldsymbol{S}$ force at the quark level.

The spin-orbit interaction between quarks can be produced by one-gluon exchange:

$$\langle \boldsymbol{p}'|V_{LS}|\boldsymbol{p}\rangle = \frac{-i}{2m_q^2}\left(\sum_A T_1^A T_2^A\right)\frac{12\pi\alpha_s}{\boldsymbol{q}^2}\boldsymbol{S}\cdot(\boldsymbol{P}\times\boldsymbol{q}). \tag{46}$$

Fourier transforming this amplitude, one obtains the spin-orbit potential:

$$V_{LS}^{\text{OGE}}(\boldsymbol{r}) = -\frac{\alpha_s}{2m_q^2 r^3}\boldsymbol{L}\cdot\boldsymbol{S}, \tag{47}$$

where we have taken color **6** channel whose color prefactor is $\sum_A T_1^A T_2^A = 1/3$. In a $^3P_2$ state, the order of magnitude of a spin-orbit attraction between two quarks exchanging a gluon is

$$V_{LS}^{\text{OGE}}(r) = -42.5\alpha_s\left(\frac{r}{\text{fm}}\right)^{-3}\left(\frac{m_q}{300 \text{ MeV}}\right)^{-2} \text{ MeV}. \tag{48}$$

With $\alpha_s \sim 0.5$ we see that $V_{LS}^{\text{OGE}}(r \sim 1 \text{ fm})$ is comparable to the aforementioned value of Eq. (45).

Alternatively, consider NJL-type models that describe the quasiparticle nature of quarks in the presence of spontaneously broken chiral symmetry. Such models have frequently been used in extrapolations to high density matter. We refer to a recent version that includes scalar and vector couplings together with diquark correlations [18,36]:

$$\mathcal{L}_{\text{int}} = G(\bar{q}q)^2 + H(\bar{q}\,\bar{q})(qq) - G_V(\bar{q}\gamma^\mu q)^2. \tag{49}$$

This model is guided by the quark-hadron continuity hypothesis and designed to meet the stiffness conditions on the EoS of dense matter imposed by the existence of heavy (two-solar-mass) neutron stars and gravitational wave signals from neutron star merger events. It features a strongly repulsive vector interaction with a coupling strength G_V comparable in magnitude to the scalar coupling G which in turn produces a "constituent" quark mass of about 0.3 GeV starting from almost massless u and d quarks. Typical values of coupling strengths are

$$G \simeq 2\Lambda^{-2}, \quad \Lambda \simeq 0.6 \text{ GeV}, \quad G_V = (0.6-1.3)G. \tag{50}$$

In the following we shall use $G_V \simeq G$ for guidance.

The scalar and vector interactions in Eq. (49) generate spin-orbit forces between quarks. In order to compare with the previous discussion for neutrons, it is useful to associate the characteristic NJL cutoff Λ with a mass scale in a bosonized version of Eq. (49) involving scalar and vector boson fields, $\sigma(x)$ and $v^\mu(x)$:

$$\mathcal{L}_S = -\tilde{g}_S\bar{q}(x)q(x)\sigma(x),$$
$$\mathcal{L}_V = -\tilde{g}_V\bar{q}(x)\gamma_\mu q(x)v^\mu(x). \tag{51}$$

For example, the scalar field satisfies

$$(\boldsymbol{\nabla}^2 - \Lambda^2)\sigma(x) = \tilde{g}_S\bar{q}(x)q(x), \tag{52}$$

so that $\sigma = -(\tilde{g}_S/\Lambda^2)\bar{q}q$ and $G = \tilde{g}_S^2/\Lambda^2$ in the long-wavelength limit. Writing the scalar field as an expectation value plus a fluctuating part, $\sigma(x) = \langle\sigma\rangle + s(x)$, it is the expectation value $\langle\sigma\rangle = -(\tilde{g}_S/\Lambda^2)\langle\bar{q}q\rangle$ that determines the constituent quark mass through the NJL gap equation, $m_q = -2G\langle\bar{q}q\rangle$, while the fluctuating part $s(x)$ propagates between quark sources and generates exchange interactions.

The spin-orbit interaction between quarks produced by the scalar and vector couplings (51) is

$$\langle \boldsymbol{p}'|V_{LS}|\boldsymbol{p}\rangle = -\frac{i}{2m_q^2}\left[\frac{\tilde{g}_S^2 + 3\tilde{g}_V^2}{\boldsymbol{q}^2 + \Lambda^2}\right]\boldsymbol{S}\cdot(\boldsymbol{P}\times\boldsymbol{q}). \tag{53}$$

By comparison with Eq. (43) it becomes evident that the spin-orbit forces between two neutrons and between two d-quarks are of the same order of magnitude: with inclusion of the isoscalar vector coupling in the neutron case (i.e., omitting the isovector vector interaction for which there is no obvious NJL counterpart) we have, roughly,

$$\frac{\tilde{g}_S^2 + 3\tilde{g}_V^2}{m_q^2\Lambda^2} \sim \frac{g_S^2 + 3g_V^2}{m_N^2 m_V^2}. \tag{54}$$

This correspondence can be further illustrated by converting Eq. (53) into an equivalent spin-orbit potential in r-space, now operating between constituent quarks:

$$V_{LS}^{qq}(\boldsymbol{r}) = \frac{1}{2m_q^2 r}\frac{df(r)}{dr}\boldsymbol{L}\cdot\boldsymbol{S},$$
$$f(r) = \frac{(\tilde{g}_S^2 + 3\tilde{g}_V^2)e^{-\Lambda r}}{4\pi r}. \tag{55}$$

For example, two d-quarks in a $^3P_2$ state and at a distance $r \sim 0.8$ fm experience a spin-orbit attraction of

$$V_{LS}^{dd}(r \sim 0.8 \text{ fm}) \simeq -16 \text{ MeV}, \qquad (56)$$

to be compared with Eq. (45). The values in the $^3P_0$ and $^3P_1$ channels are $+32$ and $+16$ MeV, respectively. Correspondingly larger magnitudes for the spin-orbit potential result if one takes the stronger vector coupling, $G_V = 1.3G$ instead of $G_V = G$.

We can conclude that spin-orbit interactions between nucleons have a close correspondence to spin-orbit interactions between quark quasiparticles emerging from NJL-type models with strong vector couplings. One can also see that spin-orbit interactions between quarks arising from one-gluon exchange reach a comparable magnitude. As a consequence, the $^3P_2$ neutron superfluidity scenario in neutron star matter has an analog in a similarly favored $^3P_2$ superfluid pairing of d-quarks at high baryon densities.

VI. SUPPORTING ARGUMENTS

We are proposing a novel phase, 2SC+$\langle dd \rangle$, which inevitably arises from the viewpoint of continuity to superfluid neutron matter. The existence of such an additional component $\langle dd \rangle$ is suggested by further independent arguments. Here we discuss the rearrangement of diquark interaction terms and the neutron star cooling phenomenology.

A. Coupling to the energy-momentum tensor

In the context of previous mean-field calculations of color-superconducting quark matter in an NJL-type model (see, e.g., Refs. [51,52] for a review), a four-fermion coupling in the $^3P_2$ channel has so far been missing. It would then be instructive to see how the interaction in this channel could be enlarged through the coupling to the energy-momentum tensor in an explicit manner. Let us consider the four-fermion coupling in the $^3P_2$ diquark channel, i.e.,

$$\hat{\mathcal{I}}_P = (\bar{\psi}\gamma^i\nabla^j\mathcal{C}\bar{\psi}^\top)(\psi^\top\mathcal{C}\gamma_i\nabla_j\psi)$$
$$= (\gamma^i\mathcal{C})_{\sigma\sigma'}(\mathcal{C}\gamma_i)_{\tau'\tau}\bar{\psi}_\sigma(\nabla^j\psi)_\tau(\nabla_j\bar{\psi})_{\sigma'}\psi_{\tau'}, \qquad (57)$$

where $\sigma, \tau, \ldots$ are spin indices.

Using the Fierz transformation matrix given explicitly in Appendix, the Fierz-rearranged four-fermion coupling is found in the form

$$\hat{\mathcal{I}}_P = -\frac{3}{4}(\bar{\psi}\nabla^j\psi)^2 - \frac{3}{4}(\bar{\psi}\gamma^0\nabla^j\psi)^2 - \frac{1}{4}(\bar{\psi}\gamma^i\nabla^j\psi)^2$$
$$+ \frac{1}{4}(\bar{\psi}\sigma^{i0}\nabla^j\psi)^2 - \frac{1}{8}(\bar{\psi}\sigma^{ij}\nabla^k\psi)^2 + \frac{3}{4}(\bar{\psi}\gamma^0\gamma^5\nabla^j\psi)^2$$
$$+ \frac{1}{4}(\bar{\psi}\gamma^i\gamma^5\nabla^j\psi)^2 - \frac{3}{4}(\bar{\psi}i\gamma^5\nabla^j\psi)^2, \qquad (58)$$

where we have introduced the compact notation $(\bar{\psi}\Gamma\nabla^j\psi)^2$ for $(\bar{\psi}\Gamma\vec{\nabla}^j\psi)(\bar{\psi}\bar{\vec{\nabla}}_j\Gamma\psi)$ in each of the terms on the right-hand side.

Notably, this Fierz transformed $\hat{\mathcal{I}}_P$ has a direct correspondence to the energy-momentum tensor in the fermionic sector, $T^{\mu\nu} = \bar{\psi}i\gamma^\mu\partial^\nu\psi$. For matter in equilibrium, $T^{\mu\nu} = \text{diag}[\varepsilon, -p, -p, -p]$, with the energy density ε and the pressure p of fermionic matter. The tree-level expectation value of $\hat{\mathcal{I}}_P$ in Eq. (58) thus becomes

$$\langle\hat{\mathcal{I}}_P\rangle \approx \frac{3}{4}p^2. \qquad (59)$$

It is evident from this algebraic exercise that the $^3P_2$ diquark interaction couples to the pressure which is a macroscopic quantity. Even if the direct mixing between the quark-antiquark (hole) and the diquark sectors may not be large, the superfluid energy gap can be enhanced by the macroscopic expectation value of the energy-momentum tensor as given in Eq. (59). Here, we also make a remark about a gauge-invariant description of the $^3P_2$ diquark condensate. To form a gauge-invariant quantity the color indices are saturated, and as long as $\langle\hat{\mathcal{I}}_P\rangle \neq 0$ as in Eq. (59) and the quark-hadron continuity is postulated, the $^3P_2$ diquark condensate squared is always mixed with the energy-momentum tensor squared through $\langle\hat{\mathcal{I}}_P\rangle \neq 0$.

B. Aspects of neutron star cooling phenomenology

The temperature of a neutron star and its time evolution (cooling), which can be read off from the thermal radiation from the stellar surface, provides information about processes occurring in the interior. A salient feature of the mechanisms behind neutron star cooling is their sensitivity to possible quark degrees of freedom inside the stellar core.

In attempts to describe the actual neutron star cooling data, pure 2SC quark matter turns out not to work [53]. This is due to the onset of the quark direct Urca process, which strongly affects the cooling curve of the star. If we assume pure 2SC matter only, some u- and d-quarks are not paired and remain as a normal component as mentioned in Sec. III B. Thus these residual quarks in the normal phase emit neutrinos via the direct Urca process and efficiently induce cooling of the star. Once the stellar mass exceeds a critical value for which the quark direct Urca process sets in, the star cools too fast.

This too fast cooling can be avoided by the formation of a condensate in the ungapped modes, here, a $\langle dd \rangle$-condensate. The existence of the superfluid gap Δ suppresses either direct or modified Urca process by the factor $\propto e^{-\Delta/T}$. Still, there remain unpaired u-quarks, but these also turn out not to contribute dominantly to the cooling: these unpaired quarks can in principle undergo the quark modified Urca process, via the charged-current interaction, and the quark bremsstrahlung process, with emission of

neutrino-antineutrino pairs, via the neutral-current interaction. However, while the former mechanism is suppressed by the superfluid gap as mentioned above, the latter process is also parametrically suppressed by the factor $\propto (T/\mu)^2$. Therefore, the formation of $\langle dd \rangle$ suppresses the fast cooling induced by the emergence of quarks inside stars.

This trend is in accord with Ref. [53] introducing *ad hoc* an additional species X with a hypothetical density-dependent pairing gap, Δ_X, so that "2SC + X" matter fits the empirically observed cooling data (at the status of 2005). This additional weak pairing channel needs to have a small gap Δ_X ranging between 10 keV and 1 MeV.

One can speculate that $^1S_0$ or $^3P_2$ superfluidity of d-quarks with its gap proportional to $\langle dd \rangle$ might be a natural candidate to substitute for the unknown X. The typical magnitude of the neutron $^3P_2$ gap is $\Delta_{nn} \sim 0.1$ MeV [54,55] (see also the recent review [24]). As we have pointed out in Sec. V B, the attractive components of spin-orbit forces between two neutrons or two d-quarks are of similar magnitude, so that one can expect a gap, Δ_{dd} of order 10–100 keV, also for d-quark pairing. This would be in accordance with the postulated properties of X. Further justification by calculating Δ_{dd} microscopically is left for future studies.

VII. SUMMARY AND CONCLUSIONS

Quark-hadron continuity postulates a soft crossover from hadronic to quark degrees of freedom in cold and dense baryonic matter if the symmetry-breaking patterns in the hadronic and quark domains are identical. Under these conditions there is no phase transition from hadrons to quarks. This scenario has been rigorously formulated for the idealized case of matter composed of three massless (u, d, s) quark flavors. The special situation with $N_F = N_C = 3$ implies color-flavor locked (CFL) configurations of diquark condensates. The CFL phase of quark matter has the same symmetry-breaking pattern as the corresponding three-flavor hadronic phase with a baryonic superfluid. As part of this joint pattern, chiral symmetry is spontaneously broken in both hadronic and quark phases.

Explicit chiral symmetry breaking by the nonzero quark masses in QCD separates the heavier strange quark from the light u and d quarks. The composition of cold matter in the real world is therefore governed by u and d quarks with their approximate isospin symmetry. Matter exists in the form of nuclei, and in the form of neutron stars at higher baryon densities. Idealized three-flavor matter is not the preferred ground state. The strange matter hypothesis is not ruled out here, but given the empirical stiffness constraints for the neutron star equation-of-state, we relegate its possibility to even higher density scales. One can then raise the question whether matter with two-flavor symmetry is still characterized by quark-hadron continuity, or whether the symmetry breaking patterns in hadronic matter versus quark matter are fundamentally different so that they are separated by a phase transition.

The present work addresses this issue for the case of neutron matter and comes to the conclusion that quark-hadron continuity can indeed be realized in such a two-flavor system. The key to this conclusion comes from a detailed investigation of superfluidity in both hadronic and quark phases. Dense matter in the core of neutron stars serves as a prototype example.

In neutron matter at low densities, the attractive S-wave interaction between neutrons at the Fermi surface generates $^1S_0$ superfluidity. At higher densities the S-wave interaction turns repulsive and $^3P_2$ neutron superfluidity takes over, driven by the attractive spin-orbit interaction in this channel. The prime question from the viewpoint of quark-hadron continuity is whether, at even higher densities, $^3P_2$ superfluidity has an analog in quark matter such that the associated order parameter can be translated continuously from one phase of matter to the other. In the preceding sections of this paper we have explored symmetry aspects and dynamical mechanisms related to this issue. The basic results are the following:

(i) Formal rearrangements including all relevant symmetries permit a systematic translation from dibaryonic operators to diquark operators and their respective condensates, for both two- and three-flavor symmetric matter.

(ii) For the interesting case of neutron matter, it is shown that superfluidity involving neutron pairs, $\langle nn \rangle$, transforms into the superfluid pairing of d-quarks, $\langle dd \rangle$, together with the formation of $\langle ud \rangle$ diquark condensates.

(iii) The strong short-range repulsion in the interaction of two neutrons has an analog in the repulsive short-distance force between two d-quarks. This mechanism disfavors S-wave superfluidity of d-quarks at high density, in the same way as it disfavors $^1S_0$ neutron superfluidity at baryon densities larger than about half the density of normal nuclear matter.

(iv) The strong spin-orbit interaction between nucleons has an analogous counterpart in a corresponding $\boldsymbol{L} \cdot \boldsymbol{S}$ force in the quark sector, generated by one-gluon exchange or by vector couplings of quarks as they appear, for example, in extended Nambu–Jona-Lasinio models. The spin-orbit forces between two neutrons as well as between two d-quarks are attractive in the triplet P-wave channel with total angular momentum $J = 2$. Therefore $^3P_2$ superfluidity in neutron matter finds its direct correspondence in $^3P_2$ superfluidity produced by d-quark pairing in quark matter.

Altogether these findings suggest the presence of identical symmetry breaking patterns, and hence quark-hadron continuity, in the transition from neutron matter to two-flavor quark matter. The new element in this case is the

continuity of $^3P_2$ superfluidity between the hadronic and the quark phase. The associated order parameter involves a tensor combination of spin and momentum. The corresponding $^3P_2$ four-fermion coupling has not been considered in previous quark matter studies. It offers novel perspectives, such as its close connection to the pressure component of the energy-momentum tensor, a macroscopic quantity. The $^3P_2$ superfluidity is also of interest in the context of neutron star cooling. It would be important to study how our continuity scenario fits within the QCD phase diagram. An interesting possibility would be a continuity scenario between the $^3P_2$ superfluidity and crystalline color-superconducting states. These and related topics are to be explored in future studies.

ACKNOWLEDGMENTS

APPENDIX: FIERZ TRANSFORMATION

The Fierz transformation matrix used in the derivations of relations in Sec. VI A is displayed here in its explicit form for the convenience of readers. For further details, readers can consult Appendix A of Ref. [51].

The relevant Fierz identity is given in a matrix form as

$$
\mathcal{D} =
\begin{pmatrix}
-\frac{1}{4} & \frac{1}{4} & \frac{1}{4} & \frac{1}{4} & \frac{1}{4} & \frac{1}{4} & \frac{1}{4} & \frac{1}{4} \\
-\frac{1}{4} & \frac{1}{4} & -\frac{1}{4} & -\frac{1}{4} & \frac{1}{4} & -\frac{1}{4} & \frac{1}{4} & -\frac{1}{4} \\
-\frac{3}{4} & -\frac{3}{4} & -\frac{1}{4} & \frac{1}{4} & -\frac{1}{4} & \frac{3}{4} & \frac{1}{4} & -\frac{3}{4} \\
-\frac{3}{4} & -\frac{3}{4} & \frac{1}{4} & -\frac{1}{4} & -\frac{1}{4} & -\frac{3}{4} & \frac{1}{4} & \frac{3}{4} \\
-\frac{3}{4} & \frac{3}{4} & -\frac{1}{4} & -\frac{1}{4} & -\frac{1}{4} & \frac{3}{4} & -\frac{1}{4} & \frac{3}{4} \\
\frac{1}{4} & \frac{1}{4} & -\frac{1}{4} & \frac{1}{4} & -\frac{1}{4} & -\frac{1}{4} & \frac{1}{4} & \frac{1}{4} \\
\frac{3}{4} & -\frac{3}{4} & -\frac{1}{4} & -\frac{1}{4} & \frac{1}{4} & \frac{3}{4} & \frac{1}{4} & \frac{3}{4} \\
\frac{1}{4} & \frac{1}{4} & \frac{1}{4} & -\frac{1}{4} & -\frac{1}{4} & \frac{1}{4} & \frac{1}{4} & -\frac{1}{4}
\end{pmatrix}
\Gamma, \quad \text{(A1)}
$$

where the diquark and the quark-antiquark (hole) interaction channels are

$$
\mathcal{D} =
\begin{pmatrix}
\mathcal{C}_{\sigma\sigma'}\mathcal{C}_{\tau'\tau} \\
(\gamma^0\mathcal{C})_{\sigma\sigma'}(\mathcal{C}\gamma^0)_{\tau'\tau} \\
(\gamma^i\mathcal{C})_{\sigma\sigma'}(\mathcal{C}\gamma_i)_{\tau'\tau} \\
(\sigma^{i0}\mathcal{C})_{\sigma\sigma'}(\mathcal{C}\sigma_{i0})_{\tau'\tau} \\
\frac{1}{2}(\sigma^{ij}\mathcal{C})_{\sigma\sigma'}(\mathcal{C}\sigma_{ij})_{\tau'\tau} \\
(\gamma^0\gamma^5\mathcal{C})_{\sigma\sigma'}(\mathcal{C}\gamma^0\gamma^5)_{\tau'\tau} \\
(\gamma^i\gamma^5\mathcal{C})_{\sigma\sigma'}(\mathcal{C}\gamma_i\gamma^5)_{\tau'\tau} \\
(i\gamma^5\mathcal{C})_{\sigma\sigma'}(i\mathcal{C}\gamma^5)_{\tau'\tau}
\end{pmatrix},
\quad
\Gamma =
\begin{pmatrix}
(\mathbf{1})_{\sigma\tau}(\mathbf{1})_{\sigma'\tau'} \\
(\gamma^0)_{\sigma\tau}(\gamma^0)_{\sigma'\tau'} \\
(\gamma^i)_{\sigma\tau}(\gamma_i)_{\sigma'\tau'} \\
(\sigma^{i0})_{\sigma\tau}(\sigma_{i0})_{\sigma'\tau'} \\
\frac{1}{2}(\sigma^{ij})_{\sigma\tau}(\sigma_{ij})_{\sigma'\tau'} \\
(\gamma^0\gamma^5)_{\sigma\tau}(\gamma^0\gamma^5)_{\sigma'\tau'} \\
(\gamma^i\gamma^5)_{\sigma\tau}(\gamma_i\gamma^5)_{\sigma'\tau'} \\
(i\gamma^5)_{\sigma\tau}(i\gamma^5)_{\sigma'\tau'}
\end{pmatrix}.
$$
$$\text{(A2)}$$

Taking the inverse of the above matrix, we can immediately derive an identity to reexpress the diquark interaction in terms of the quark-antiquark (hole) interaction. In this way we can read the matrix elements to derive a translation from Eq. (57) to Eq. (58).

[1] T. Schäfer and F. Wilczek, Phys. Rev. Lett. **82**, 3956 (1999).

[2] M. G. Alford, J. Berges, and K. Rajagopal, Nucl. Phys. **B558**, 219 (1999).

[3] T. Hatsuda, M. Tachibana, N. Yamamoto, and G. Baym, Phys. Rev. Lett. **97**, 122001 (2006).

[4] H. Abuki, G. Baym, T. Hatsuda, and N. Yamamoto, Phys. Rev. D **81**, 125010 (2010).

[5] N. Yamamoto, M. Tachibana, T. Hatsuda, and G. Baym, Phys. Rev. D **76**, 074001 (2007).

[6] T. Hatsuda, M. Tachibana, and N. Yamamoto, Phys. Rev. D **78**, 011501 (2008).

[7] M. G. Alford, G. Baym, K. Fukushima, T. Hatsuda, and M. Tachibana, Phys. Rev. D **99**, 036004 (2019).

[8] C. Chatterjee, M. Nitta, and S. Yasui, Phys. Rev. D **99**, 034001 (2019).

[9] A. Cherman, S. Sen, and L. G. Yaffe, Phys. Rev. D **100**, 034015 (2019).

[10] Y. Hirono and Y. Tanizaki, Phys. Rev. Lett. **122**, 212001 (2019); J. High Energy Phys. 07 (2019) 062.

[11] L. McLerran and R. D. Pisarski, Nucl. Phys. **A796**, 83 (2007).

[12] K. Fukushima and T. Kojo, Astrophys. J. **817**, 180 (2016).

[13] L. McLerran and S. Reddy, Phys. Rev. Lett. **122**, 122701 (2019).

[14] K. S. Jeong, L. McLerran, and S. Sen, Phys. Rev. C **101**, 035201 (2020).

[15] K. Masuda, T. Hatsuda, and T. Takatsuka, Astrophys. J. **764**, 12 (2013).

[16] D. E. Alvarez-Castillo, S. Benic, D. Blaschke, and R. Łastowiecki, Acta Phys. Pol. B Proc. Suppl. **7**, 203 (2014).

[17] G. Baym, T. Hatsuda, T. Kojo, P. D. Powell, Y. Song, and T. Takatsuka, Rep. Prog. Phys. **81**, 056902 (2018).

[18] G. Baym, S. Furusawa, T. Hatsuda, T. Kojo, and H. Togashi, Astrophys. J. **885**, 42 (2019).

[19] Y. Fujimoto, K. Fukushima, and K. Murase, Phys. Rev. D **98**, 023019 (2018); **101**, 054016 (2020).

[20] F. Özel, G. Baym, and T. Guver, Phys. Rev. D **82**, 101301 (2010); F. Ozel, D. Psaltis, Z. Arzoumanian, S. Morsink, and M. Baubock, Astrophys. J. **832**, 92 (2016).

[21] A. W. Steiner, J. M. Lattimer, and E. F. Brown, Astrophys. J. **722**, 33 (2010); **765**, L5 (2013).

[22] B. P. Abbott *et al.* (LIGO Scientific and Virgo Collaborations), Phys. Rev. Lett. **121**, 161101 (2018).

[23] A. Gezerlis, C. J. Pethick, and A. Schwenk, in *Novel Superfluids*, edited by K.-H. Bennemann and J. B. Ketterson, International Series of Monographs in Physics Vol. 2 (Oxford University Press, Oxford, 2015), p. 580.

[24] A. Sedrakian and J. W. Clark, Eur. Phys. J. A **55**, 167 (2019).

[25] M. Hoffberg, A. E. Glassgold, R. W. Richardson, and M. Ruderman, Phys. Rev. Lett. **24**, 775 (1970).

[26] R. Tamagaki, Prog. Theor. Phys. **44**, 905 (1970); T. Takatsuka and R. Tamagaki, Prog. Theor. Phys. Suppl. **112**, 27 (1993).

[27] P. F. Bedaque, G. Rupak, and M. J. Savage, Phys. Rev. C **68**, 065802 (2003).

[28] K. Masuda and M. Nitta, Phys. Rev. C **93**, 035804 (2016).

[29] G. Watanabe and C. J. Pethick, Phys. Rev. Lett. **119**, 062701 (2017).

[30] C. Drischler, T. Krüger, K. Hebeler, and A. Schwenk, Phys. Rev. C **95**, 024302 (2017).

[31] M. Kitazawa, T. Koide, T. Kunihiro, and Y. Nemoto, Prog. Theor. Phys. **108**, 929 (2002); **110**, 185(E) (2003).

[32] Z. Zhang, K. Fukushima, and T. Kunihiro, Phys. Rev. D **79**, 014004 (2009).

[33] V. D. Burkert, L. Elouadrhiri, and F. X. Girod, Nature (London) **557**, 396 (2018).

[34] E. Fonseca *et al.*, Astrophys. J. **832**, 167 (2016); J. Antoniadis *et al.*, Science **340**, 1233232 (2013); H. T. Cromartie *et al.*, Nat. Astron. **4**, 72 (2020).

[35] M. Drews and W. Weise, Prog. Part. Nucl. Phys. **93**, 69 (2017).

[36] Y. Song, G. Baym, T. Hatsuda, and T. Kojo, Phys. Rev. D **100**, 034018 (2019).

[37] F. Wilczek, in *From Fields to Strings: Circumnavigating Theoretical Physics. Ian Kogan Memorial Collection (3 Volume Set)* (World Scientific, Singapore, 2004), pp. 322–338; R. L. Jaffe, Phys. Rep. **409**, 1 (2005).

[38] Strictly speaking, Eq. (13) is only valid for the good diquark. Two quarks in **3** representation of color and flavor group reduce to $\mathbf{3} \times \mathbf{3} = \bar{\mathbf{3}} + \mathbf{6}$. The indices on the right-hand side of Eq. (13) are those of **3**, while on the left-hand side they refer to $\bar{\mathbf{3}}$ after the reduction. Namely, by this definition, we are only taking out the color-antisymmetric and the flavor-antisymmetric part ($\bar{\mathbf{3}}$) of the complete diquark operator. See also Eqs. (14) and (16).

[39] R. Casalbuoni and R. Gatto, Phys. Lett. B **464**, 111 (1999).

[40] D. T. Son and M. A. Stephanov, Phys. Rev. D **61**, 074012 (2000); **62**, 059902(E) (2000).

[41] J. Berges and K. Rajagopal, Nucl. Phys. **B538**, 215 (1999); M. Huang, P.-f. Zhuang, and W.-q. Chao, Phys. Rev. D **65**, 076012 (2002).

[42] C. Ratti and W. Weise, Phys. Rev. D **70**, 054013 (2004).

[43] M. G. Alford, J. A. Bowers, J. M. Cheyne, and G. A. Cowan, Phys. Rev. D **67**, 054018 (2003).

[44] M. G. Alford, H. Nishimura, and A. Sedrakian, Phys. Rev. C **90**, 055205 (2014).

[45] D. Bailin and A. Love, Phys. Rep. **107**, 325 (1984).

[46] M. Oka and K. Yazaki, Phys. Lett. **90B**, 41 (1980).

[47] M. Oka and K. Yazaki, Prog. Theor. Phys. **66**, 556 (1981); **66**, 572 (1981).

[48] A. De Rujula, H. Georgi, and S. L. Glashow, Phys. Rev. D **12**, 147 (1975).

[49] M. M. Nagels, T. A. Rijken, and J. J. de Swart, Phys. Rev. D **12**, 744 (1975).

[50] R. Machleidt, K. Holinde, and C. Elster, Phys. Rep. **149**, 1 (1987).

[51] M. Buballa, Phys. Rep. **407**, 205 (2005).

[52] M. G. Alford, A. Schmitt, K. Rajagopal, and T. Schäfer, Rev. Mod. Phys. **80**, 1455 (2008).

[53] H. Grigorian, D. Blaschke, and D. Voskresensky, Phys. Rev. C **71**, 045801 (2005).

[54] M. Baldo, O. Elgaroey, L. Engvik, M. Hjorth-Jensen, and H. J. Schulze, Phys. Rev. C **58**, 1921 (1998).

[55] D. Ding, A. Rios, H. Dussan, W. H. Dickhoff, S. J. Witte, A. Polls, and A. Carbone, Phys. Rev. C **94**, 025802 (2016); **94**, 029901(A) (2016).